

# Index-Based Concatenated Codes for the Multi-Draw DNA Storage Channel

Lorenz Welter\*, Issam Maarouf<sup>†</sup>, Andreas Lenz\*,  
Antonia Wachter-Zeh\*, Eirik Rosnes<sup>†</sup>, and Alexandre Graell i Amat<sup>‡</sup>

\*School of Computation, Information and Technology, Technical University of Munich, DE-80333 Munich, Germany

<sup>†</sup>Simula UiB, N-5006 Bergen, Norway

<sup>‡</sup>Department of Electrical Engineering, Chalmers University of Technology, SE-41296 Gothenburg, Sweden

**Abstract**—We consider error-correcting coding for DNA-based storage. We model the DNA storage channel as a *multi-draw IDS channel* where the input data is chunked into  $M$  short DNA strands, which are copied a random number of times, and the channel outputs a random selection of  $N$  noisy DNA strands. The retrieved DNA strands are prone to insertion, deletion, and substitution (IDS) errors. We propose an index-based concatenated coding scheme consisting of the concatenation of an outer code, an index code, and an inner *synchronization* code, where the latter two tackle IDS errors. We further propose a mismatched joint index-synchronization code maximum a posteriori probability decoder with optional clustering to infer symbolwise a posteriori probabilities for the outer decoder. We compute achievable information rates for the outer code and present Monte-Carlo simulations for information-outage probabilities and frame error rates on synthetic and experimental data, respectively.

## I. INTRODUCTION

This work aims at improving the reliability of DNA-based data storage. We analyze the *multi-draw IDS channel* which is an abstraction of the synthesis (writing), storage, and sequencing (reading) procedures, including insertion, deletion, and substitution (IDS) errors, thereby narrowing the modeling gap to the real DNA storage channel [1].

The capacity of the DNA storage channel has been studied in [2]–[5]; see [6] for an overview. For coping with IDS errors in a single-sequence transmission, the classical scheme in [7] with the improved decoding method from [8] is most relevant for our work. Independently, [9], [10] analyzed coded trace reconstruction under IDS errors and showed significant gains by leveraging multiple noisy copies of the same transmit sequence even with sub-optimal decoding techniques.

Inspired by experimental works [11]–[16], we propose an index-based concatenated coding scheme for the multi-draw IDS channel. Index-based schemes for the multi-draw IDS channel are sub-optimal, albeit very practical [6], [17]. Similar coding approaches are analyzed in [18], [19]. In our scheme, the information is encoded by an outer code to provide overall error protection, primarily coping with unresolved errors and strand erasures of the data. The resulting codeword is split into  $M$  data blocks. In each data block, index information is embedded after being encoded by a low-rate index code, whereas the data block itself is encoded by an inner code. Both codes are tailored to deal with IDS errors. The  $M$  resulting strands are then transmitted over the multi-draw IDS channel,

The work of L. Welter, A. Lenz, and A. Wachter-Zeh has been supported by the European Research Council (ERC) under the European Union’s Horizon 2020 research and innovation programme (Grant Agreement No. 801434).

The work of A. Graell i Amat was supported by the Swedish Research Council under grant 2020-03687.

which models the DNA storage channel. At the receiver, each noisy strand is decoded separately by a joint index and inner maximum a posteriori probability (MAP) decoder outputting symbolwise a posteriori probabilities (APPs). To leverage the multi-copy gain, we combine the APPs according to the subsequent clustering and index decoding. We optionally cluster the received strands based on the obtained APPs, benefiting from the error-correction capabilities of the index and inner codes. For each cluster, an index decision is made by jointly considering the received strands in a cluster. The APPs are ordered according to the index decisions and fed into a soft-input outer decoder.

We analyze our proposed scheme in terms of achievable information rates (AIRs). The AIRs provide insights to the performance of different index-inner coding and decoding techniques and a benchmark for an outer code. For different coding setups in the finite blocklength regime, we compute information-outage probabilities on synthetic data and present frame error rates (FERs) on experimental data from [9].

## II. DNA STORAGE CHANNEL MODEL

### A. IDS Channel

We consider a model in which IDS errors are independent and identically distributed. Let  $\mathbf{x} = (x_1, \dots, x_L)$  and  $\mathbf{y} = (y_1, \dots, y_{L'})$  be the DNA strand to be synthesized and a single read at the output of the sequencing process, respectively, with  $x_t, y_t \in \Sigma_4 = \{A, C, G, T\}$ .

The input to the channel can be seen as a queue in which symbols  $x_t$  are successively enqueued for transmission. The output strand  $\mathbf{y}$  is generated as follows:  $\mathbf{y}$  is first initialized to an empty vector before  $x_1$  is enqueued. Then, for each input symbol  $x_t$ , the following three events may occur: 1) A random symbol  $a \in \Sigma_4$  is inserted with probability  $p_I$ . In this case,  $\mathbf{y}$  is concatenated with symbol  $a$  as  $\mathbf{y} \leftarrow (\mathbf{y}, a)$  and  $x_t$  remains in the queue. 2) The symbol  $x_t$  is deleted with probability  $p_D$ ,  $\mathbf{y}$  remains unchanged, and  $x_{t+1}$  is enqueued. 3) The symbol  $x_t$  is transmitted with probability  $p_T = 1 - p_I - p_D$ . In this case, the symbol is received correctly with probability  $1 - p_S$  or incorrectly with probability  $p_S$ , in which case the symbol is substituted by a symbol  $a' \in \Sigma_4 \setminus \{x_t\}$  picked uniformly at random. The output is set to  $\mathbf{y} \leftarrow (\mathbf{y}, x_t)$  and  $\mathbf{y} \leftarrow (\mathbf{y}, a')$ , respectively, and  $x_{t+1}$  is enqueued. After  $x_L$  leaves the queue, we obtain the output strand  $\mathbf{y}$ , of length  $L'$ . Note that  $L'$  is random and depends on the channel realization. Further, the symbols in  $\mathbf{y}$  are not synchronized anymore. Hence,  $y_t$  could be the result of transmitting a symbol  $x_{t'}$  with  $t' \neq t$ .

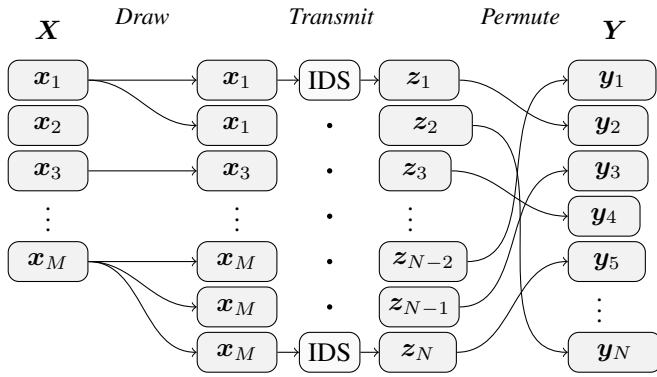


Fig. 1. Multi-draw IDS channel.

### B. Multi-Draw IDS Channel

The data sequence is divided into  $M$  short DNA strands  $\mathbf{x}_1, \dots, \mathbf{x}_M$ , each of length  $L$ , which are synthesized and stored in a *pool*. We define the input list  $\mathbf{X} \triangleq (\mathbf{x}_1, \dots, \mathbf{x}_M)$ . We assume that the PCR amplification and sequencing processes generate  $N = cM$  reads from the strands in the pool, resulting in a random number of (noisy) reads for each strand  $\mathbf{x}_i$ . The factor  $c$  is a positive real number referred to as the *coverage depth* in the literature.

The channel between the input to be synthesized,  $\mathbf{X}$ , and the output of the sequencing process,  $\mathbf{Y}$ , can be modeled in three phases as explained in the following.

- 1) *Draw*:  $N$  draws are performed from the list  $\mathbf{X}$  uniformly at random with replacement. Let  $D_i$  be the random variable (RV) corresponding to the number of times strand  $\mathbf{x}_i$  is drawn and define the random vector  $\mathbf{D} \triangleq (D_1, \dots, D_M)$ , with  $\sum_i D_i = N$ . Then, the random vector  $\mathbf{D} = (D_1, \dots, D_M)$  is multinomially distributed as  $\mathbf{D} \sim \text{Multinom}(M, N, 1/M)$ .
- 2) *Transmit*: The drawn strands are transmitted through independent IDS channels with identical parameters  $p_I$ ,  $p_D$ , and  $p_S$ . We denote by  $\mathbf{z}_j$  the output of the  $j$ -th IDS channel,  $j \in \{1, \dots, N\}$ , and define  $\mathbf{Z} \triangleq (\mathbf{z}_1, \dots, \mathbf{z}_N)$ .
- 3) *Permute*: The final output of the channel, denoted as the list  $\mathbf{Y} \triangleq (\mathbf{y}_1, \dots, \mathbf{y}_N)$  is obtained by a permutation of  $\mathbf{Z}$  chosen uniformly at random.

We illustrate the channel model in Fig. 1.<sup>1</sup> We define the channel parameter  $\beta = \frac{\log_4(M)}{L}$  that relates the total number and the length of the strands and can be interpreted as the penalty the channel induces by the permutation effect.

### III. INDEX-BASED CONCATENATED CODING SCHEME

We propose an index-based concatenated coding scheme consisting of three codes: an outer spatially-coupled low-density parity-check (SC-LDPC) code, providing overall protection to the data and against non-drawn strands, an index code, which counteracts the loss of ordering in the presence of IDS errors, and an inner code whose main goal is to maintain synchronization.

<sup>1</sup>In [3], [5], [6], the *draw* and *permute* steps are considered as a joint process referred to as *sampling*. We split the step for the sake of presentation; our channel model is essentially the same channel model, only that we consider the noise channel to be an IDS channel.

The information  $\mathbf{u} \in \mathbb{F}_4^{k_o}$  is encoded by an  $[n_o, k_o, \frac{M}{2}, m]_4$  SC-LDPC code of output length  $n_o$ , input length  $k_o$ , coupling length  $\frac{M}{2}$ , and coupling memory  $m$  over the field  $\mathbb{F}_4$  [20], [21]. Note that there is a one-to-one mapping of the field  $\mathbb{F}_4$  to the DNA alphabet  $\Sigma_4 = \{A, C, G, T\}$ . We interpret it as a field to allow linear operations over vectors in the DNA alphabet. The resulting codeword  $\mathbf{w} = (w_1, \dots, w_{n_o}) \in \mathbb{F}_4^{n_o}$  is split into  $M$  equal-length data blocks as  $\mathbf{w} = (\mathbf{w}^{(1)}, \dots, \mathbf{w}^{(M)})$  such that  $\mathbf{w}^{(i)} = (w_1^{(i)}, \dots, w_{L_o}^{(i)}) \in \mathbb{F}_4^{L_o}$ ,  $L_o = \frac{n_o}{M}$ . Each index  $i$  is encoded by an  $[n_{ix}, k_{ix}]_4$  index code over  $\mathbb{F}_4$  of even output length  $n_{ix}$  and even input length  $k_{ix} \geq \log_4(M)$  to an index codeword. Independently, the data block  $\mathbf{w}^{(i)}$  is encoded by an  $[n_i, k_i]_4$  inner code over  $\mathbb{F}_4$  of output length  $n_i$ , input length  $k_i$ , and rate  $R_i = \frac{k_i}{n_i}$ , generating an inner data codeword of length  $\frac{L_o}{R_i}$ . We consider the marker-repeat (MR) codes presented in [9], [22] for the inner code, where the  $k_i$ -th input symbol is repeated once such that  $n_i = k_i + 1$  and  $R_i = 1 - \frac{1}{n_i}$ . Due to our decoding technique, we have higher error protection at the beginning and end of the DNA strands. Thus, we split the index codeword in half and insert it at the beginning and the end of the inner codeword of the respective data block. Finally, a random offset sequence is added to the generated strand resulting in the final encoded output strand  $\mathbf{x}_i$ , of length  $L = L_o R_i^{-1} + n_{ix}$ . The random offset is known to the decoder and supports the synchronization capability of the index and inner decoder and ensures that the nucleotides of the stored DNA strands are uniformly distributed over  $\Sigma_4$ . The final codeword list is then described by  $\mathbf{X} = (\mathbf{x}_1, \dots, \mathbf{x}_M)$ . The overall code rate is  $R = 2 \cdot R_o \frac{L_o}{L}$  in bits/nucleotide, with individual rates  $R_o = \frac{k_o}{n_o}$ ,  $R_{ix} = \frac{k_{ix}}{n_{ix}}$ , and recall  $R_i = \frac{k_i}{n_i}$ .

For the decoding procedure we introduce the following equivalent interpretation of the index and inner encoding as a joint process. We transform the integer  $i$  to a vector  $\text{ind}(i) \in \mathbb{F}_4^{k_{ix}}$ . This vector is split in half and placed at the beginning and end of the vector  $\mathbf{w}^{(i)}$  resulting in the vector  $\mathbf{v}^{(i)} = (v_1^{(i)}, \dots, v_{k_{ix}+L_o}^{(i)})$ , of length  $k_{ix} + L_o$ . Moreover, the  $[n_{ix}, k_{ix}]_4$  index code is generated by a serial concatenation of two equal  $[\frac{n_{ix}}{2}, \frac{k_{ix}}{2}]_4$  codes. Subsequently, the vector  $\mathbf{v}^{(i)}$  is encoded at the index positions by the  $[\frac{n_{ix}}{2}, \frac{k_{ix}}{2}]_4$  code and symbolwise by the inner MR code at the positions corresponding to  $\mathbf{w}^{(i)}$ . The coding/decoding scheme is depicted in Fig. 2.

### IV. JOINT INDEX AND INNER DECODING

The channel introduces two main impairments that need to be combated: the loss of ordering of the DNA strands due to the permutation effect, and the possibility that a strand is not drawn due to the drawing nature. However, the latter also provides inherent redundancy due to possible multiple copies of the same DNA strand that can be leveraged. Moreover, at the receiver side, the loss of synchronization within each strand due to insertion and deletion events is challenging. In general, we follow a *mismatched decoding* approach due to the decoder's channel uncertainty and complexity constraints. Instead of considering all DNA strands in the received list  $\mathbf{Y}$  jointly to produce an estimate of the information,  $\hat{\mathbf{u}}$ , we propose the following sub-optimal decoding scheme.

First, we infer symbolwise APPs using a joint index and inner MAP decoder by means of the BCJR algorithm for

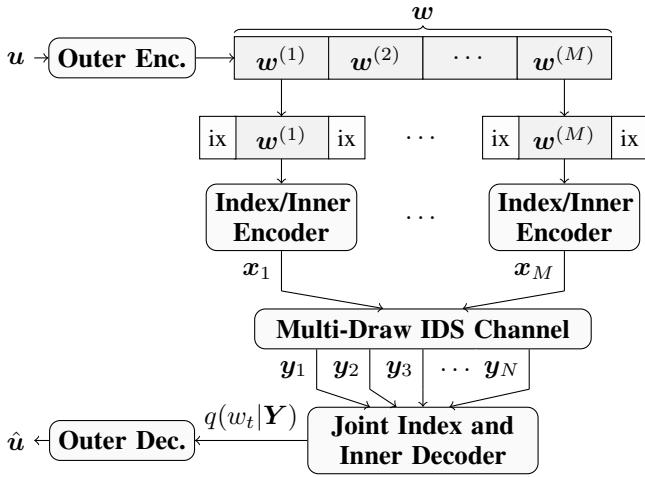


Fig. 2. Concatenated coding scheme for the communication over the multi-draw IDS channel. The index is split into two parts and is inserted at the beginning and the end of the block  $w^{(i)}$ . The term  $q(w_t|\mathbf{Y})$  denotes the mismatched metric computed by the joint index-inner decoder.

each received strand  $\mathbf{y}_1, \dots, \mathbf{y}_N$  independently. Optionally, clustering of the DNA strands using the APPs is performed. In that way the clustering makes use of the coding gain provided by the index and inner code. For combining the APPs within a cluster, the APPs are symbolwise multiplied, generating the mismatched APPs for one cluster. For a given cluster, by making hard-decisions on the index APPs, we estimate the block index  $\hat{i}$  within  $\mathbf{w}$ . Therefore, assuming optimal clustering, we can actually benefit from the multi-copy gain of the channel for the index estimation. Once more, the APPs of the data block belonging to the same index  $\hat{i}$  are multiplied, generating the mismatched APPs  $q(w_t^{(\hat{i})}|\mathbf{Y})$ . The overall ordered APPs  $q(w_t|\mathbf{Y})$  are then passed to the outer decoder, which neglects any possible correlations of the symbolwise APPs. The outer code is specifically designed to handle *block-fading* effects, as described in Section VI. Combining APPs after inner and before outer decoding by symbolwise multiplication is inspired by the well performing *separate decoding* strategy of [10].

### A. Inner MAP Decoding

We consider the case of decoding a single output strand  $\mathbf{y}$  given an input  $\mathbf{v}$  by means of the BCJR decoder over the joint code trellis of the index and inner code. We drop the superscript of the sequence  $\mathbf{v}$  due to the permutation effect of the channel. We follow the concept introduced in [7], refined in [8]. For a detailed view, we refer to our prior work [10].

The IDS errors introduce a synchronization loss that destroys the Markov property of the joint index-inner code. However, we can form a hidden Markov model by introducing the drift  $d_t$ , defined as the number of insertions minus the number of deletions that occurred at time  $t$ , as a hidden state variable. The essence of the drift states is that the sequence  $d_0, \dots, d_{L_o+k_{ix}}$  forms a Markov chain and the outputs after time  $t+1$  are independent of the previous states, restoring the Markov property. Hence, we can formulate forward and backward recursions for a BCJR decoder, whose final output APPs are  $p(v_t|\mathbf{y}) = \frac{p(v_t, \mathbf{y})}{p(\mathbf{y})} \propto \sum_{d, d'} p(v_t, \mathbf{y}, d, d')$ , where  $d$  and  $d'$  denote realizations of the RVs  $d_t$  and  $d_{t+1}$ , respectively.

### B. Clustering

Common approaches perform clustering on the received strands before error-correction decoding using approximation techniques for the Levenshtein distance (minimum number of IDS operations), e.g., [16], [23]. Here, we present a clustering approach of complexity  $\mathcal{O}(N^2L)$  that leverages the coding gain of the index and inner code.

Given the APPs  $p(v_t|\mathbf{y}_j)$ , for each strand  $\mathbf{y}_j$  a vector  $\mathbf{r}^{(j)} = (r_1^{(j)}, \dots, r_{L_B}^{(j)}) \in \mathbb{R}^{L_B}$  of binary log-likelihood ratios (LLRs) is obtained using marginalization, where  $\mathbb{R}$  denotes the reals and  $L_B$  is the length of the corresponding binary vector of  $\mathbf{v}$ . The clustering decision is made by evaluating the pairwise Euclidean distance

$$d_E^{(i,j)} = \sqrt{\sum_{\ell=1}^{L_B} (r_\ell^{(i)} - r_\ell^{(j)})^2}$$

for any two vectors  $\mathbf{r}^{(i)}$  and  $\mathbf{r}^{(j)}$ ,  $i \neq j$ . Let  $D_E^{\text{intra}}$  be the RV of the Euclidean distance between two received sequences  $\mathbf{r}^{(i)}$  and  $\mathbf{r}^{(j)}$  originating from the same stored DNA strand. Assuming no correlations between the binary LLRs,  $D_E^{\text{intra}}$  converges asymptotically in  $L_B$  to a normal distribution  $\mathcal{N}(\mu_D, \sigma_D^2)$  with mean  $\mu_D$  and variance  $\sigma_D^2$  [24]. By sampling realizations of  $D_E^{\text{intra}}$ , it can be observed that this is a good approximation for  $L_B > 100$  for fitted parameters  $\mu_D$  and  $\sigma_D^2$ . Consequently, given the computed pairwise distances  $d_E^{(i,j)}$  for  $i, j \in \{1, \dots, N\}$ ,  $i \neq j$ , strands are considered to stem from the same DNA strand if  $d_E^{(i,j)} \leq \mu_D + \omega \cdot \sigma_D$ , where  $\omega \in \mathbb{R}^+$  is a design parameter and  $\mathbb{R}^+$  denotes the set of positive real numbers.

Let the  $k$ -th cluster,  $1 \leq k \leq M'$ , be formed as  $\mathbf{C}_k \triangleq (\mathbf{y}_{k,1}, \dots, \mathbf{y}_{k,|\mathbf{C}_k|})$ , where  $\mathbf{y}_{k,j}$  is the  $j$ -th strand placed in cluster  $\mathbf{C}_k$  and  $|\mathbf{C}_k| \neq 0$ . Denote the overall clustering output as the list  $\mathbf{C} = (\mathbf{C}_1, \dots, \mathbf{C}_{M'})$ , with  $1 \leq M' \leq N$  and  $\sum_{k=1}^{M'} |\mathbf{C}_k| = N$ . For each cluster  $k$ , we multiply the respective APPs giving the mismatched rule

$$q(v_t|\mathbf{C}_k) \propto \prod_{j=1}^{|\mathbf{C}_k|} \frac{p(v_t|\mathbf{y}_{k,j})}{p(v_t)^{|\mathbf{C}_k|-1}}.$$

### C. Index and Multiple DNA Strand Decoding

The index code and recovering the index information of each strand/cluster at the receiver side is the key point of tackling the permutation effect and leveraging the multi-copy gain of the channel. For each cluster  $\mathbf{C}_k$ , we obtain the soft information of the indices by extracting

$$\mathbf{q}(\text{ind}(i)|\mathbf{C}_k) \triangleq (q(v_1|\mathbf{C}_k), \dots, q(v_{k_{ix}/2}|\mathbf{C}_k), \\ q(v_{L_o+k_{ix}/2+1}|\mathbf{C}_k), \dots, q(v_{L_o+k_{ix}}|\mathbf{C}_k)).$$

We perform hard-decisions on  $\mathbf{q}(\text{ind}(i)|\mathbf{C}_k)$  to compute an estimate index  $\hat{i}_k$  for every cluster  $1 \leq k \leq M'$ , which will determine how the strand/cluster is grouped. Let  $\mathcal{S}_i$  be the set of clusters with decision on index  $i$ , where  $0 \leq |\mathcal{S}_i| \leq M'$ . For all data positions of the  $i$ -th block, i.e., for symbols of  $\mathbf{w}^{(i)}$ , we compute the APPs according to the mismatched rule

$$q(w_t^{(i)}|\mathbf{Y}) \propto \prod_{k \in \mathcal{S}_i} \frac{q(w_t^{(i)}|\mathbf{C}_k)}{q(w_t^{(i)})^{|\mathcal{S}_i|-1}},$$

where  $q(w_t^{(i)}|\mathbf{Y}) = \frac{1}{4}$  when  $\mathcal{S}_i = \emptyset$ .

As a final step, according to the position of block  $w^{(i)}$  in the sequence  $w$ , the mismatched APPs are given to the outer decoder, which outputs an estimate  $\hat{u}$ .

## V. ACHIEVABLE INFORMATION RATES

We compute AIRs of mismatched decoders for fixed index and inner codes. Specifically, we compute i.u.d. *BCJR-once* rates ( $R_{\text{BCJR-once}}$ ), measured in bits/nucleotide, which are defined as the symbolwise mutual information between the input and its corresponding LLRs with uniform input distribution [25]–[27]. The BCJR-once rates serve as an appropriate measure of an AIR for an outer decoder that ignores possible correlations between the symbolwise estimates  $q(w_t|\mathbf{Y})$  given by the inner MAP decoder. Moreover, by using a mismatched decoding metric  $q(w|\mathbf{Y})$  instead of the true metric  $p(w|\mathbf{Y})$ , the rate  $R_{\text{BCJR-once}}$  only decreases. Consider the mismatched-decoder decoding metric

$$q(w|\mathbf{Y}) = \prod_{i=1}^M \prod_{t=1}^{L_o} q(w_t^{(i)}|\mathbf{Y}).$$

The mutual information  $I(w; \mathbf{Y})$  can be bounded from below as (for clarity of presentation, we do not distinguish between RVs and their realizations in our notation)

$$I(w; \mathbf{Y}) \geq \mathbb{E}_{\mathcal{D}} \left[ \sum_{i,t} \mathbb{E}_{w_t^{(i)}, \mathbf{Y}|\mathcal{D}} \left[ \log_2 \frac{q(w_t^{(i)}|\mathbf{Y})}{p(w_t^{(i)})} \right] \right],$$

where  $\mathbb{E}_X[\cdot]$  denotes expectation with respect to the RV  $X$ .

We define the LLR representation

$$\text{LLR}_{i,t}(a) = \sum_{k \in \mathcal{S}_i} \sum_{j=1}^{|\mathcal{C}_k|} \ln \frac{q(w_t^{(i)} = a | \mathbf{y}_{k,j})}{q(w_t^{(i)} = 0 | \mathbf{y}_{k,j})},$$

where  $\mathbf{y}_{k,j}$  denotes the  $j$ -th strand of  $\mathcal{C}_k$ . Similar to [25], we use the mismatched LLR representation to formally define

$$R_{\text{BCJR-once}} \triangleq \mathbb{E}_{\mathcal{D}} \left[ \lim_{ML \rightarrow \infty} \frac{1}{ML} \sum_{i=1}^M \sum_{t=1}^{L_o} I(w_t^{(i)}; \text{LLR}_{i,t}(w_t^{(i)})) \right],$$

which depends on the multi-draw parameters  $\beta$  and  $c$ , IDS channel parameters  $p_I$ ,  $p_D$ , and  $p_S$ , and is evaluated for a fixed index and inner coding/decoding scheme. Assuming ergodicity for a single strand, we follow a simulation-based approach to calculate  $R_{\text{BCJR-once}}$ . We simulate for long strand lengths  $\tilde{L} = 100\,000$  (correspondingly  $\tilde{L}_o = (\tilde{L} - n_{ix})R_i$  and  $\tilde{M} = 4^{\beta\tilde{L}}$ ), reflecting  $ML \rightarrow \infty$  for a fixed  $\beta$ , and approximate  $\mathbb{E}_{\mathcal{D}}[\cdot]$  by the Monte-Carlo method. Hence, by averaging over a large number of draw realizations,  $\Phi$ , we approximate  $R_{\text{BCJR-once}}$  as

$$R_{\text{BCJR-once}} \approx \frac{1}{\Phi} \sum_{\phi=1}^{\Phi} \frac{1}{ML} \sum_{i=1}^{\tilde{M}} \sum_{t=1}^{\tilde{L}_o} \left( \log_2 4 + \log_2 \frac{e^{\text{LLR}_{i,t}(w_t^{(i)})}}{\sum_{a \in \mathbb{F}_4} e^{\text{LLR}_{i,t}(a)}} \right).$$

## VI. OUTER CODE

Due to its drawing effect, the DNA storage channel as seen by the outer code resembles a block-fading channel when considering a finite number of strands  $M$  [5]. Hence, it also shares its afflictions, most importantly its non-ergodic property. In particular, an *outage* event occurs when not enough strands are

drawn for a specific block. Formally, an outage event occurs when the instantaneous mutual information between the input and output of the channel is lower than the transmission rate  $R_o$ . We consider the BCJR-once version of the information-outage probability adapted from [28], to which we refer as the *mismatched information-outage probability*  $q_{\text{out}}$ . It incorporates our mismatched decoding approach, the fixed i.u.d. input, and the dispersion due to the finite blocklength phenomena. Let  $r_{\text{BCJR-once}}^d$  denote the instantaneous BCJR-once information density for the finite length regime and fixed draw realization  $d$ , computed as

$$r_{\text{BCJR-once}}^d = \frac{1}{ML} \sum_{i=1}^M \sum_{t=1}^{L_o} I(w_t^{(i)}; \text{LLR}_{i,t}(w_t^{(i)})).$$

Then,  $q_{\text{out}}$  is formally defined as

$$q_{\text{out}} = \Pr(r_{\text{BCJR-once}}^d < R'_o) \geq p_{\text{out}},$$

where  $R'_o = 2R_o$  such that the outer code rate is measured in bits/nucleotide and  $p_{\text{out}}$  is the true outage probability.  $q_{\text{out}}$  gives a lower bound on the FER for a given encoder and mismatched decoder pair, i.e., using the mismatched metric described Section V, for fixed finite number of strands, fixed finite blocklength, and fixed channel parameters. We approximate  $q_{\text{out}}$  by the Monte-Carlo method for a given  $R'_o$ .

The diversity order of the outer code is an important parameter that influences the slope of the FER curve for low IDS probabilities. By coding over blocks of  $w$ , the outer code can provide a *diversity* gain. We consider protograph-based SC-LDPC codes for the outer code, as they achieve high diversity for the block-fading channel [29]. We optimize the protograph following the procedure in [29] based on the density evolution outage (DEO) probability bound. The optimization works by first finding a block LDPC protograph with DEO close to a target  $q_{\text{out}} = 10^{-3}$  based on the joint index-inner code. Then, an optimization over the edge spreading to create the SC-LDPC protograph is performed. In order to design a non-binary code, random edge weights from  $\mathbb{F}_4$  are assigned to the edges of the protograph throughout the optimization. In the optimization, we fix the coupling length to  $\frac{M}{2}$  and the coupling memory to  $m = 2$ .

## VII. AIR AND FER RESULTS

We analyze our proposed coding scheme for the multi-draw IDS channel by means of AIRs, information-outage probability for the outer code, and FER simulations for different coverage depths  $c$  and fixed  $\beta$ . We set the IDS channel parameters to  $p_I = 0.017$ ,  $p_D = 0.020$ , and  $p_S = 0.022$ , motivated by the results of the experiment from [9]. Additionally, we present FER results on their experimental data. Moreover, we fix the inner code rate to  $R_i = \frac{10}{11}$  and perform full-window belief propagation decoding with a maximum of 100 iterations for the SC-LDPC outer code. The index codes  $[3, 1]_4$  (AIR simulations) and  $[6, 2]_4$  (information-outage/FER simulations), both with  $R_{ix} = \frac{1}{3}$ , are obtained via an exhaustive graph search algorithm optimizing the code's Levenshtein distance spectrum (see Table I) [10], [30].

Fig. 3 shows the AIR  $R_{\text{BCJR-once}}$  of different coding/decoding schemes for  $\beta = 2 \cdot 10^{-5}$ . We observe the unavoidable rate loss due to the non-drawing strand and permutation effect for low coverage depth  $c$  which, however,

TABLE I  
INDEX CODES

Code	Codebook
$[3, 1]_4$	(0, 3, 3), (1, 0, 2), (2, 1, 1), (3, 2, 0)
$[6, 2]_4$	(0, 0, 1, 0, 1, 1), (0, 0, 3, 3, 2, 2), (0, 2, 2, 2, 2, 0), (1, 1, 1, 0, 2, 3), (1, 1, 2, 2, 0, 1), (1, 1, 3, 3, 3, 0), (1, 3, 0, 3, 1, 1), (2, 0, 1, 1, 0, 0), (2, 0, 3, 2, 3, 3), (2, 2, 2, 0, 3, 2), (2, 2, 3, 1, 1, 1), (2, 3, 0, 2, 2, 2), (3, 1, 0, 1, 3, 3), (3, 1, 1, 2, 1, 2), (3, 3, 2, 1, 1, 0), (3, 3, 3, 0, 0, 3)

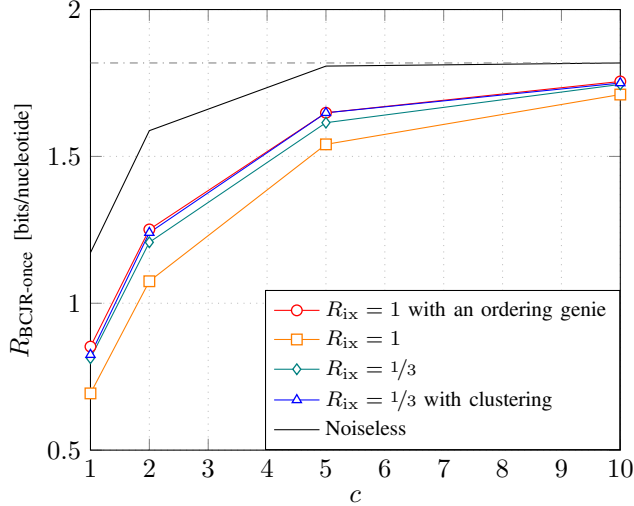


Fig. 3. BCJR-once rates versus coverage depth  $c$  for different index coding rates  $R_{ix}$  and decoding techniques. Fixed parameters are  $\beta = 2 \cdot 10^{-5}$ ,  $p_I = 0.017$ ,  $p_D = 0.020$ ,  $p_S = 0.022$ , and  $R_i = \frac{10}{11}$ . For clustering, we determined  $D_E^{intra} \sim \mathcal{N}(938, 6.4^2)$  and use  $\omega = 5$ . The dash-dotted gray line represents the rate limit due to the inner code rate.

diminishes for increasing values of  $c$  due to the multi-copy gain. For an overall benchmark, we include the AIR of an optimal index-based scheme over the noiseless channel (i.e., only drawing and permuting effects). With IDS noise, we include a benchmark for an index-based coding approach given an index genie in the decoding process, i.e., we artificially exclude the permutation loss of the channel. The rate gap to the noiseless scenario can be explained by the IDS noise and is also due to our chosen sub-optimal coding and mismatched decoding approach. Moreover, protecting the index with a strong code seems crucial since in the non-coded case received strands may be grouped incorrectly. For the given parameters, the designed index code performs very close to the genie ordering curve, while the non-coded index curve suffers from a big rate loss. Further, applying our clustering method in combination with a coded index attains the index genie benchmark since the clustering enhances the quality of the index decisions.

Fig. 4 shows the information-outage probability  $q_{out}$  versus the outer code rate  $R'_o = 2R_o$  for different coverage depths  $c$  and decoding approaches for  $M = 256$  input strands and fixed index code of rate  $R_{ix} = \frac{1}{3}$ . For a fixed  $R'_o$ , the corresponding  $q_{out}$  serves as a lower bound for any code's FER with that rate and length, and a decoder following our mismatched decoding rule. In general, we see a similar behavior of our proposed coding/decoding schemes as for the AIRs. In the same figure, we show the FER performance of a protograph-based SC-LDPC outer code (stand-alone solid shaped markers). The SC-LDPC protograph is optimized individually for each considered coding/decoding scheme and then randomly

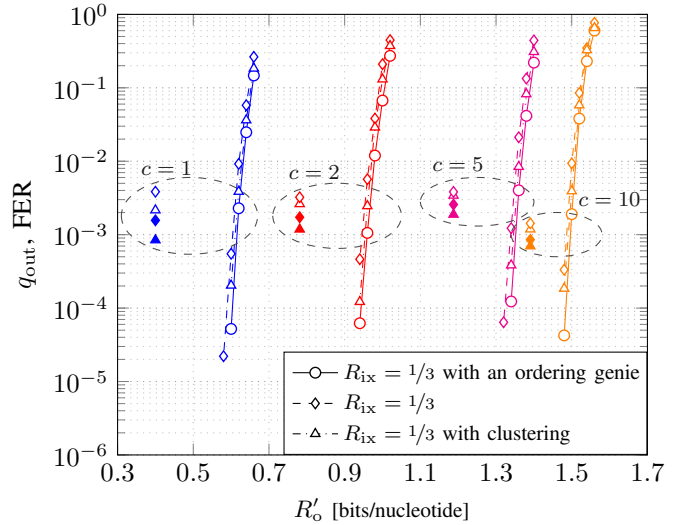


Fig. 4. Information-outage probability  $q_{out}$  and FER versus outer code rate  $R'_o = 2R_o$ , for fixed  $n_o = 23040$ ,  $M = 256$ ,  $L = 110$ ,  $\beta \approx 0.36$ ,  $p_I = 0.017$ ,  $p_D = 0.020$ ,  $p_S = 0.022$ , and  $R_i = 0.9183 \approx \frac{10}{11}$ . For clustering, we determined  $D_E^{intra} \sim \mathcal{N}(31.52, 5.44^2)$  and use  $\omega = 2.5$ . The different curves represent  $q_{out}$  for different coding/decoding schemes. The stand-alone markers correspond to the FER performance when using an optimized SC-LDPC outer code on synthetic (solid shaped) and experimental (empty shaped) data.

TABLE II  
BLOCK LDPC PHOTOGRAPHS FOR DIFFERENT VALUES OF  $c$

$c$	Protograph <sup>a</sup>		$R'_o$
	Coded-index	Coded-index + clustering	
1	$\begin{pmatrix} 1 & 1 & 1 & 0 & 1 \\ 1 & 1 & 1 & 1 & 0 \\ 1 & 0 & 1 & 0 & 1 \\ 0 & 1 & 0 & 2 & 0 \end{pmatrix}$	$\begin{pmatrix} 1 & 1 & 1 & 0 & 1 \\ 0 & 0 & 2 & 2 & 0 \\ 2 & 0 & 0 & 0 & 1 \\ 0 & 2 & 0 & 1 & 0 \end{pmatrix}$	0.3750
2	$\begin{pmatrix} 1 & 2 & 0 & 0 & 1 \\ 0 & 0 & 1 & 1 & 1 \\ 2 & 1 & 2 & 1 & 0 \end{pmatrix}$	$\begin{pmatrix} 1 & 1 & 0 & 1 & 0 \\ 1 & 0 & 2 & 1 & 1 \\ 1 & 2 & 1 & 0 & 1 \end{pmatrix}$	0.7812
5	$\begin{pmatrix} 2 & 1 & 0 & 2 & 2 \\ 0 & 2 & 2 & 1 & 1 \end{pmatrix}$	$\begin{pmatrix} 2 & 1 & 0 & 2 & 2 \\ 0 & 2 & 2 & 1 & 1 \end{pmatrix}$	1.1876
10	$\begin{pmatrix} 1 & 2 & 1 & 1 & 0 & 0 & 0 & 1 & 1 & 2 \\ 1 & 0 & 2 & 0 & 2 & 1 & 2 & 0 & 1 & 0 \\ 0 & 1 & 0 & 1 & 1 & 2 & 0 & 2 & 1 & 1 \end{pmatrix}$	$\begin{pmatrix} 1 & 1 & 1 & 1 & 0 & 0 & 0 & 1 & 2 & 1 \\ 1 & 1 & 0 & 0 & 2 & 1 & 2 & 2 & 0 & 1 \\ 0 & 1 & 2 & 1 & 1 & 2 & 0 & 0 & 1 & 1 \end{pmatrix}$	1.3906

<sup>a</sup>Optimized edge spreading is performed on the given protographs, with a coupling length of 128 and a coupling memory of  $m = 2$ . Recall  $R'_o = 2R_o$ .

lifted and assigned random edge weights from  $\mathbb{F}_4$ . We observe an expected rate loss that can be explained by the limited protograph search space. The corresponding optimized (block) LDPC photographs are shown in Table II. Finally, we also include FER results on experimental data from [9] (stand-alone empty shaped markers). Notably, the penalty in performance, due to the fact that the experimental channel may suffer from other additional noise impairments, is small. In addition, the SC-LDPC photographs are optimized on synthetic samples and not on experimental data which also contributes to the loss in performance.

## VIII. CONCLUSION

We proposed a practical index-based concatenated coding scheme for the multi-draw IDS channel, a model approximating the DNA storage process. Further, we presented low-complexity decoding techniques for this setup. Our AIR results show that, in the presence of IDS errors, protecting the index with a strong code is crucial. Finally, we proposed explicit code constructions with FER performance of around  $10^{-3}$  for synthetic and experimental data and 256 input strands.

## REFERENCES

- [1] R. Heckel, G. Mikutis, and R. N. Grass, "A characterization of the DNA data storage channel," *Sci. Rep.*, vol. 9, no. 9663, pp. 1–12, Jul. 2019.
- [2] R. Heckel, I. Shomorony, K. Ramchandran, and D. N. C. Tse, "Fundamental limits of DNA storage systems," in *Proc. IEEE Int. Symp. Inf. Theory*, Aachen, Germany, Jun. 2017.
- [3] A. Lenz, P. H. Siegel, A. Wachter-Zeh, and E. Yaakobi, "An upper bound on the capacity of the DNA storage channel," in *Proc. IEEE Inf. Theory Workshop*, Visby, Sweden, Aug. 2019.
- [4] ———, "Achieving the capacity of the DNA storage channel," in *Proc. IEEE Int. Conf. Acoust., Speech, Sig. Process.*, Barcelona, Spain, May 2020.
- [5] N. Weinberger and N. Merhav, "The DNA storage channel: Capacity and error probability bounds," *IEEE Trans. Inf. Theory*, vol. 68, no. 9, pp. 5657–5700, Sep. 2022.
- [6] I. Shomorony and R. Heckel, "Information-theoretic foundations of DNA data storage," *Found. Trends Commun. Inf. Theory*, vol. 19, no. 1, pp. 1–106, Feb. 2022.
- [7] M. C. Davey and D. J. C. MacKay, "Reliable communication over channels with insertions, deletions, and substitutions," *IEEE Trans. Inf. Theory*, vol. 47, no. 2, pp. 687–698, Feb. 2001.
- [8] J. A. Briffa, H. G. Schaathun, and S. Wesemeyer, "An improved decoding algorithm for the Davey-MacKay construction," in *Proc. IEEE Int. Conf. Commun.*, Cape Town, South Africa, May 2010.
- [9] S. R. Srinivasavaradhan, S. Gopi, H. D. Pfister, and S. Yekhanin, "Trellis BMA: Coded trace reconstruction on IDS channels for DNA storage," in *Proc. IEEE Int. Symp. Inf. Theory*, Melbourne, Australia, Jul. 2021.
- [10] I. Maarouf, A. Lenz, L. Welter, A. Wachter-Zeh, E. Rosnes, and A. Graell i Amat, "Concatenated codes for multiple reads of a DNA sequence," *IEEE Trans. Inf. Theory*, vol. 69, no. 2, pp. 910–927, Feb. 2023.
- [11] G. M. Church, Y. Gao, and S. Kosuri, "Next-generation digital information storage in DNA," *Sci.*, vol. 337, no. 6102, p. 1628, Aug. 2012.
- [12] N. Goldman, P. Bertone, S. Chen, C. Dessimoz, E. M. LeProust, B. Sipos, and E. Birney, "Towards practical, high-capacity, low-maintenance information storage in synthesized DNA," *Nature*, vol. 494, no. 7435, pp. 77–80, Jan. 2013.
- [13] R. N. Grass, R. Heckel, M. Puddu, D. Paunescu, and W. J. Stark, "Robust chemical preservation of digital information on DNA in silica with error-correcting codes," *Angew. Chem. Int. Ed.*, vol. 54, no. 8, pp. 2552–2555, Feb. 2015.
- [14] S. M. H. T. Yazdi, Y. Yuan, J. Ma, H. Zhao, and O. Milenkovic, "A rewritable, random-access DNA-based storage system," *Sci. Rep.*, vol. 5, no. 14138, pp. 1–10, Sep. 2015.
- [15] L. Organick, S. D. Ang, Y.-J. Chen, R. Lopez, S. Yekhanin, K. Makarychev, M. Z. Racz, G. Kamath, P. Gopalan, B. Nguyen, C. N. Takahashi, S. Newman, H.-Y. Parker, C. Rashtchian, K. Stewart, G. Gupta, R. Carlson, J. Mulligan, D. Carmean, G. Seelig, L. Ceze, and K. Strauss, "Random access in large-scale DNA data storage," *Nature Biotechnol.*, vol. 36, no. 3, pp. 242–248, Mar. 2018.
- [16] P. L. Antkowiak, J. Lietard, M. Z. Darestani, M. M. Somoza, W. J. Stark, R. Heckel, and R. N. Grass, "Low cost DNA data storage using photolithographic synthesis and advanced information reconstruction and error correction," *Nature Commun.*, vol. 11, no. 5345, pp. 1–10, Oct. 2020.
- [17] A. Lenz, P. H. Siegel, A. Wachter-Zeh, and E. Yaakobi, "Coding over sets for DNA storage," *IEEE Trans. Inf. Theory*, vol. 66, no. 4, pp. 2331–2351, Apr. 2020.
- [18] A. Lenz, L. Welter, and S. Puchinger, "Achievable rates of concatenated codes in DNA storage under substitution errors," in *Proc. IEEE Int. Symp. Inf. Theory Appl.*, Kapolei, USA, Oct. 2020.
- [19] N. Weinberger, "Error probability bounds for coded-index DNA storage systems," *IEEE Trans. Inf. Theory*, vol. 68, no. 11, pp. 7005–7022, Nov. 2022.
- [20] A. J. Felström and K. S. Zigangirov, "Time-varying periodic convolutional codes with low-density parity-check matrix," *IEEE Trans. Inf. Theory*, vol. 45, no. 6, pp. 2181–2191, Sep. 1999.
- [21] M. Lentmaier, A. Sridharan, D. J. Costello, Jr., and K. S. Zigangirov, "Iterative decoding threshold analysis for LDPC convolutional codes," *IEEE Trans. Inf. Theory*, vol. 56, no. 10, pp. 5274–5289, Oct. 2010.
- [22] M. Inoue and H. Kaneko, "Adaptive synchronization marker for insertion/deletion/substitution error correction," in *Proc. IEEE Int. Symp. Inf. Theory*, Cambridge, USA, Jul. 2012.
- [23] C. Rashtchian, K. Makarychev, M. Rác, S. D. Ang, D. Jevdjic, S. Yekhanin, L. Ceze, and K. Strauss, "Clustering billions of reads for DNA data storage," in *Proc. Adv. Neural Inf. Process. Syst.*, Long Beach, USA, Dec. 2017.
- [24] B. A. Dawkins, T. T. Le, and B. A. McKinney, "Theoretical properties of distance distributions and novel metrics for nearest-neighbor feature selection," *PLOS ONE*, vol. 16, no. 2, pp. 1–67, Feb. 2021.
- [25] A. Kavčić, X. Ma, and M. Mitzenmacher, "Binary intersymbol interference channels: Gallager codes, density evolution, and code performance bounds," *IEEE Trans. Inf. Theory*, vol. 49, no. 7, pp. 1636–1652, Jul. 2003.
- [26] R. R. Müller and W. H. Gerstacker, "On the capacity loss due to separation of detection and decoding," *IEEE Trans. Inf. Theory*, vol. 50, no. 8, pp. 1769–1778, Aug. 2004.
- [27] J. B. Soriaga, H. D. Pfister, and P. H. Siegel, "Determining and approaching achievable rates of binary intersymbol interference channels using multistage decoding," *IEEE Trans. Inf. Theory*, vol. 53, no. 4, pp. 1416–1429, Apr. 2007.
- [28] D. Buckingham and M. C. Valenti, "The information-outage probability of finite-length codes over AWGN channels," in *Proc. 42nd Annu. Conf. Inf. Sci. Syst.*, Princeton, USA, Mar. 2008.
- [29] N. ul Hassan, M. Lentmaier, I. Andriyanova, and G. P. Fettweis, "Improving code diversity on block-fading channels by spatial coupling," in *Proc. IEEE Int. Symp. Inf. Theory*, Honolulu, USA, Jun./Jul. 2014.
- [30] E. C. Sewell, "A branch and bound algorithm for the stability number of a sparse graph," *INFORMS J. Comput.*, vol. 10, no. 4, pp. 438–447, Nov. 1998.